PHYSICAL REVIEW D VOLUME 44, NUMBER 4 15 AUGUST 1991

Order-to-chaos transition in SU(2) Yang-Mills-Higgs theory

Tetsuji Kawabe
Physics Department, Kyushu Institute of Design, Shiobaru, Fukuoka 815, Japan

Shonosuke Ohta
Physics Department, College of General Education, Kyushu University, Ropponmatsu, Fukuoka 810, Japan
(Received 25 October 1990; revised manuscript received 15 April 1991)

The onset of dynamical chaos is numerically studied in spherically symmetric time-dependent SU(2) Yang-Mills-Higgs theory. From the induction phenomena and the dependence of the maximal Lyapunov exponents on perturbations to the 't Hooft–Polyakov magnetic-monopole solution we find that there exists a critical value of the perturbation, below which the system is regular. Above this critical value, the phase transition from order to chaos takes place and thus the system exhibits a spatiotemporal chaos which generates a random inhomogeneity of the color fields. Various characteristics of a regular phase and a chaotic one and the configurations of the fields are investigated by means of the real time evolution of the system.

I. INTRODUCTION

Much attention has been paid in the last decade to the question of the integrability of Yang-Mills (YM) fields [1–4]. Most studies made so far have confined themselves to YM classical mechanics [1] where gauge fields depend on time alone and have revealed that this is a nonintegrable and chaotic system.

It has been recently shown that the SU(2) YM equation in $3+1$ dimensions is a nonintegrable system for the case of the time-dependent spherically symmetric solution [2–4]. Especially the phase space near the Wu-Yang magnetic-monopole solution [5] is clarified to become ergodic and chaotic under even infinitesimally small perturbation [4]. This result supports the consequence that YM classical mechanics is a Kolmogorov K system [6], which possesses the properties of ergodicity and mixing. The chaos in YM theory has been speculated to connect with the problems of the QCD vacuum and color confinement [7]. It is thus time for an analysis of a more realistic case including Higgs fields from these viewpoints.

In this paper we study numerically the chaotic properties of the 't Hooft–Polyakov magnetic-monopole solutions [8] in the SU(2) Yang-Mills-Higgs (YMH) theory. We adopt the Fermi-Pasta-Ulam approach [9] in which continuous equations are replaced by a set of discrete ones. By solving a set of the field equations in real time we first study the distribution of the mode energy among harmonics. From the pattern of the energy sharing among normal modes we show that the induction phenomenon [10] occurs at a large perturbation region. This phenomenon gives some information on the mechanism of the onset of chaos; i.e., its existence indicates that the system undergoes a thermalization and becomes ergodic. Next we calculate the maximal Lyapunov exponents [11] to judge whether or not the system is chaotic. The sign of their exponents provides a reliable criterion to distinguish between a regular system and chaos. Then we clarify the dependence of the Lyapunov exponents on the strength of the perturbation.

These analyses lead us to the remarkable consequence that there exists a phase transition in this system in the following sense: In the small perturbation to the 't Hooft–Polyakov monopole solution, the motion is regular and the system is close to the integrable one. As the strength of the perturbation increases above a critical value, the motion becomes chaotic. Since the pure SU(2) YM system is always chaotic [4], this result clarifies an interesting role of the Higgs field that tends to order the system. The existence of these two phases affects the spatiotemporal behavior of the YM field and the Higgs field.

II. FORMULATION

The Lagrangian density for the SU(2) YMH system we consider is [8]

$$L=-\tfrac{1}{4}F^{a}_{\mu\nu}F^{\mu\nu a}+\tfrac{1}{2}D_{\mu}\phi^{a}D^{\mu}\phi^{a}-V(\boldsymbol{\phi}) \ , \tag{1}$$

where $F^{a}_{\mu\nu}=\partial_{\mu}A^{a}_{\nu}-\partial_{\nu}A^{a}_{\mu}+e\varepsilon^{abc}A^{b}_{\mu}A^{c}_{\nu}$, $D_{\mu}\phi^{a}=\partial_{\mu}\phi^{a}-e\varepsilon^{abc}A^{b}_{\mu}\phi^{c}$, and the Higgs potential is $V(\boldsymbol{\phi})=(\lambda/4)(\boldsymbol{\phi}\cdot\boldsymbol{\phi}-v^{2})^{2}$. The equations of motion are

$$(D_{\nu}F^{\mu\nu})_{a}=-e\varepsilon_{abc}\phi_{b}(D^{\mu}\phi)_{c} \ , \tag{2}$$

$$(D^{\mu}D_{\mu}\phi)_{a}=-\lambda\phi_{a}(\boldsymbol{\phi}\cdot\boldsymbol{\phi}-v^{2}) \ . \tag{3}$$

Using the time-dependent 't Hooft–Polyakov ansatz [8,12] for the YM gauge field A^{a}_{μ} and the Higgs field ϕ_{a} as

$$\xi^{2}A^{a}_{i}(\xi,\tau)=-v\varepsilon_{aij}\xi_{j}[1-G(\xi,\tau)] \ , \tag{4}$$

$$\xi^{2}\phi_{a}(\xi,\tau)=-v\xi_{a}H(\xi,\tau) \ , \tag{5}$$

the above equations of motion reduce to

$$\xi^2(\partial_\tau^2-\partial_\xi^2)G=-H^2G-G(G^2-1)\ , \tag{6}$$

$$\xi^2(\partial_\tau^2-\partial_\xi^2)H=-2G^2H-\kappa H(H^2-\xi^2)\ , \tag{7}$$

where $\xi=evr$ and $\tau=evt$ denote the variables of space and time, respectively, and $\kappa=\lambda/e^2$ the coupling constant. We use the gauge $A_0^a=0$. The masses of the gauge and Higgs bosons are $M_A=ev$ and $M_H=\sqrt{2\lambda}v$, respectively, and then $\kappa=M_H^2/2M_A^2$. The total energy of the system is given by

$$E=\frac{4\pi v}{e}\int_0^\infty d\xi\left[(\partial_\tau G)^2+(\partial_\xi G)^2+\frac{1}{2\xi^2}(G^2-1)^2+\tfrac{1}{2}(\partial_\tau H)^2+\frac{1}{2\xi^2}(\xi\partial_\xi H-H)^2+\frac{G^2H^2}{\xi^2}+\frac{\kappa}{4\xi^2}(H^2-\xi^2)^2\right]. \tag{8}$$

For the numerical analysis of this SU(2) YMH system, we approximate Eqs. (6) and (7) by a set of nonlinear coupled oscillators, $G(i,\tau)$ and $H(i,\tau)$, by means of the Fermi-Pasta-Ulam method [9]. Here a discretization of space is introduced through $\xi=i\times a$ with lattice spacing a and $i=1,2,\ldots,N$. In order to study the perturbations near the static solutions $G_s(i)$ and $H_s(i)$ of the 't Hooft–Polyakov magnetic-monopole [8], we expand G and H by harmonics around the static solutions. The YM field G and the Higgs field H are given by

$$\begin{bmatrix}G(i,\tau)\\H(i,\tau)\end{bmatrix}=\begin{bmatrix}G_s(i)\\H_s(i)\end{bmatrix}+\left[\frac{2}{N}\right]^{1/2}\sum_{j=1}^{N-1}\begin{bmatrix}\psi_g(j,\tau)\\\psi_h(j,\tau)\end{bmatrix}\sin\left[\frac{\pi ij}{N}\right]. \tag{9}$$

As the boundary conditions must be imposed in order that the total energy be finite, we put

$$G(0,\tau)=1,\quad H(0,\tau)=0,\quad G(N,\tau)=0,\quad H(N,\tau)=Na\ . \tag{10}$$

The appropriate initial conditions are

$$\dot G(i,0)=0,\quad \dot H(i,0)=0\ . \tag{11}$$

III. INDUCTION PHENOMENA DUE TO ENERGY SHARING AMONG NORMAL MODES

As one of the basic indicators of the stochastic character of the system with many degrees of freedom, it is frequently used to measure the energy sharing among normal modes [9,10,13]. In this paper, we calculate them by exciting initially the mode $j=N/2$ alone of the YM field in Eq. (9), i.e., $\psi_g(N/2,0)\equiv A$ and $\psi_h(j,0)=0$ in addition to Eq. (11). The strength of the initial perturbation is thus determined by the amplitude A. In the numerical simulation we use the eighth-order Runge-Kutta routine with time-step size $\Delta t=0.03$ and space-step size $a=0.1$. This value of Δt was chosen small enough to maintain the total energy to a relative error of 10^{-3} after 10^6 iterations [14], i.e., $\tau=3\times10^4$. Similarly, the lattice spacing a was chosen so as to assure that the monopole masses calculated here were coincident with those [8,15] obtained previously to within an accuracy of 1–2 %.

Figure 1 gives examples of the time evolution of the energy sharing among 64 normal modes for $A=1.5$ and 0.1 in the YM fields and the Higgs fields with $\kappa=1.0$ and a spatial volume $N=64$. From the pattern of shade corresponding to the degree of magnitudes of energy E_j shared to the mode j, we notice several regularities for $A=0.1$ as shown in Figs. 1(a1) and 1(a2): The energy transfer occurs periodically at every 17–18 in the real-time unit between the mode 32 and its adjacent modes in the YM fields (a1), and the same periodicity is also observed in the

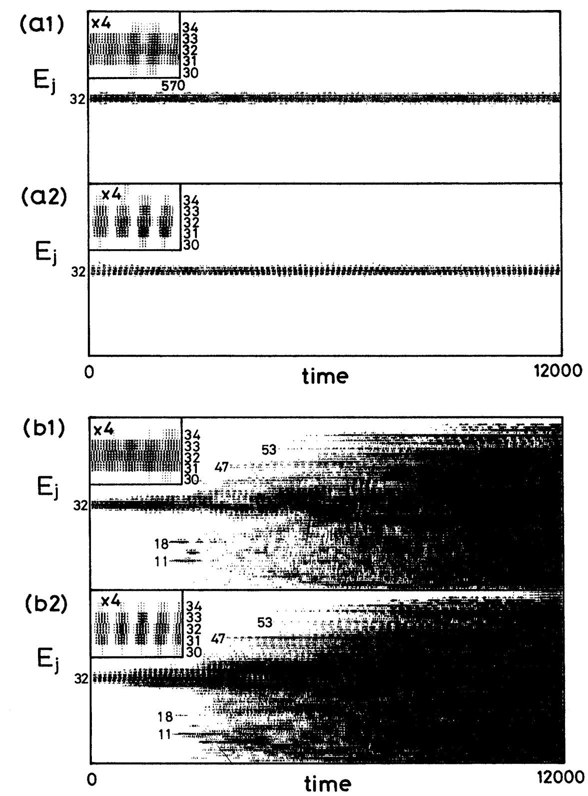

FIG. 1. Time evolution of the energy sharing of the initial mode energy E_{32} among 64 normal modes for $\kappa=1.0$ and $N=64$. Evolution in the Yang-Mills field is (a1) for $A=0.1$ and (b1) for $A=1.5$. Similarly, the evolution in the Higgs field is (a2) for $A=0.1$ and (b2) for $A=1.5$. The degree of shade corresponds to the magnitude of E_j. Vertical axis represents the mode energy E_j for $j=1-64$.

Higgs fields (a2). The coupled oscillation between both fields exists with a period $\simeq 140$. Furthermore, we observe that the energy E_{32} becomes maximum at every $\tau \simeq 6.0\times 10^3$, i.e., the recurrence takes place at this interval. Thus the motion is quasiperiodic and lies on the invariant Kolmogorov-Arnold-Moser (KAM) tori [11]. For $A=1.5$, on the other hand, the energy transfer changes among all modes chaotically after the energy sharing starts between the neighborhood of the mode 32 and other modes such as $j=11$, 18, 47, and 53 as shown in Figs. 1(b1) and 1(b2). Thus the remarkable recurrence is not observed in this case any more although we notice features similar to the case of $A=0.1$ at an early stage of time evolution.

These results suggest that in this system there exist two types of behavior depending on the magnitude of A: i.e., the quasiperiodic motion for very small A and the stochastic one for large A. In fact, we can observe the induction phenomenon [10] for $A=1.5$ which implies the system will become stochastic. This phenomenon is described as follows: The initial energy given to one normal mode remains almost unchanged during a certain amount of time T_i called an induction period, and then the energy sharing starts violently after T_i. Such a behavior can be observed for the energy E_{32} in Figs. 1(b1) and 1(b2). However, if we take into account the quasiperiodic energy transfer between the mode 32 and its neighbor, we could expect clearer behavior for the combined energies E_j composed of three modes ($j=31-33$). Indeed we can obtain a distinct induction phenomenon for such a combination of modes and measure the induction period $T_i \simeq 2.0\times 10^3$ for the YM field as shown in Fig. 2(a). Here the value of T_i is defined by the time when the energy of the excited mode is reduced to half of the initial value.

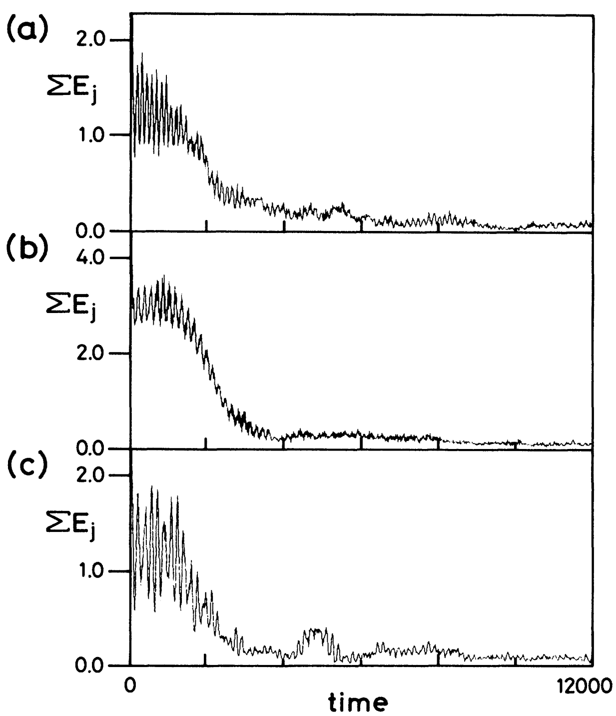

FIG. 2. Induction phenomena observed near the 't Hooft–Polyakov magnetic-monopole solution for the combined mode energies E_j with $j=N/2, N/2\pm 1$ of the Yang-Mills field with $\kappa=1.0$. (a) $A=1.5$, $a=0.1$, and $N=64$; (b) $A=\sqrt{2}\times 1.5$, $a=0.1$, and $N=128$; and (c) $A=1.5$, $a=0.4$, and $N=64$. Other modes excited after the induction period are not depicted.

In order to check whether or not these results such as recurrence times and induction phenomena strongly depend on the relatively coarse discretization and nearby boundaries, we have studied different sizes of the system. The effect of the coarse discretization and boundaries on the calculation is measured by tuning both N and a appropriately. For several sizes of the physical volume Na the values of the induction period T_i have been obtained under the same strength of the perturbation as one determined by $A=1.5$ and $N=64$ as follows: $(Na, N, a, T_i)=(3.2,64,0.05,2500)$; (6.4,32,0.2,1500), (6.4,64,0.1,2000 [Fig. 2(a)]), (6.4,128,0.05,2050); (12.8,32,0.4,2000), (12.8,64,0.2,2400), (12.8,128,0.1,2050 [Fig. 2(b)]); (25.6,32,0.8,2500), (25.6,64,0.4,1950 [Fig. 2(c)]), (25.6,128,0.2,1900); (51.2,64,0.8,2250), and (51.2,128,0.4,1600). Values of the induction period changed somewhat according to the conditions under which we carried out our numerical calculations but they seem to be reasonable convergence as the lattice spacing approaches zero for fixed physical volume. Since the monopole core has radius $\xi_{MC}\approx 1$ as will be shown in Sec. V, the maximum value of the physical volume Na we considered is almost 50 times larger than the size of the monopole. Thus the above data seem to indicate that the induction phenomena can occur after the elapse of $T_i \approx 2060$ for $A=1.5$ even at a larger volume without essentially reflecting boundary conditions. Above results, therefore, strongly suggest that the induction phenomena are not due to the discretization effects nor nearby boundaries in the SU(2) YMH equations restricted to a small volume but they are characteristic of the real dynamics of the original infinite volume equations.

IV. TWO PHASES CHARACTERIZED BY MAXIMAL LYAPUNOV EXPONENTS

Chaos comes from the property of the mixing [11]. Since the induction period is characteristic for the approach to thermal equilibrium, the SU(2) YMH system becomes ergodic after a finite time. However the ergodicity does not always imply the mixing. In order to determine whether or not our system is chaotic, we need to measure the maximal Lyapunov exponent σ. This exponent is defined as [11]

$$\sigma = \lim_{\tau\to\infty} \frac{1}{\tau} \ln \frac{d(\tau)}{d(0)} , \tag{12}$$

$$d(\tau) = \left[\sum_{k=1}^{N-1} (u'_k - u_k)^2 \right]^{1/2} , \tag{13}$$

where $d(\tau)$ is a distance between the two neighboring fields whose initial position is separated by ϵ and $u_k(i,\tau)=(G,\dot{G},H,\dot{H})$. The exponent σ is a measure of the average exponential rate of divergence of nearby trajectories in the phase space. A constant positive σ means that the system is chaotic. On the other hand, the regular motion is characterized by $\sigma=0$. Figure 3 shows several plots of the maximal Lyapunov exponents σ as function of the amplitudes A for four different values of the coupling constant κ. Here we took $\epsilon=1.0\times10^{-5}$, $a=0.1$, and $N=64$. From Fig. 3 we find that there exist the critical values $A_c\approx0.6-1.0$ for $\kappa=0.0$, 1.0, 10.0, and 50.0 at which σ becomes zero and then the system becomes regular for $A < A_c$ and chaotic for $A > A_c$.

We also have checked the dependence of σ on the coarse discretization and the physical volume. For instance, we obtained values of σ for $A=1.5$ and $\kappa=1.0$ as follows: $(Na,N,a,\sigma(\times10^3))=(6.4,32,0.2,3.09\pm0.44)$, $(6.4,64,0.1,4.92\pm0.80$ [Fig. 3(b)]), $(6.4,128,0.05,6.93\pm0.82)$, and $(12.8,128,0.1,3.19\pm1.31)$, which seems to be reasonable convergence. The magnitude of σ gives us a quantitative measure of just how chaotic it is and thus the chaotic state of our system is characterized by $\sigma\approx4.53\times10^{-3}$ for $A=1.5$ and $\kappa=1.0$. By similar analyses we obtained qualitatively the same dependence of σ on A as Fig. 3 calculated with $N=64$ and $a=0.1$.

Therefore the existence of A_c seems to be characteristic of the real dynamics of SU(2) YMH equations in infinite volume and we could expect that the phase transition from order to chaos occurs above this critical value. This result is consistent with the patterns observed in the energy sharing in Sec. III. This striking feature characterizes the SU(2) YMH system, so that this is quite different from the SU(2) YM system which is always chaotic near the Wu-Yang monopole solution for lack of A_c [4]. Our result shows that the Higgs fields are necessary to have an ordered phase in the theory.

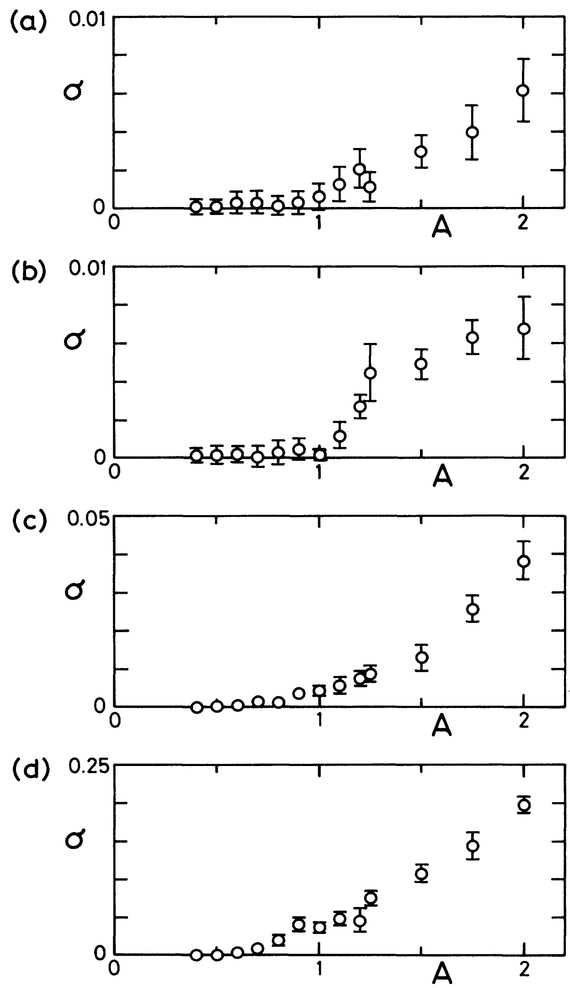

FIG. 3. Maximal Lyapunov exponents σ vs amplitudes A around the static solution of the 't Hooft–Polyakov magnetic monopole for $N=64$: (a) $\kappa=0.0$, (b) $\kappa=1.0$, (c) $\kappa=10.0$, and (d) $\kappa=50.0$.

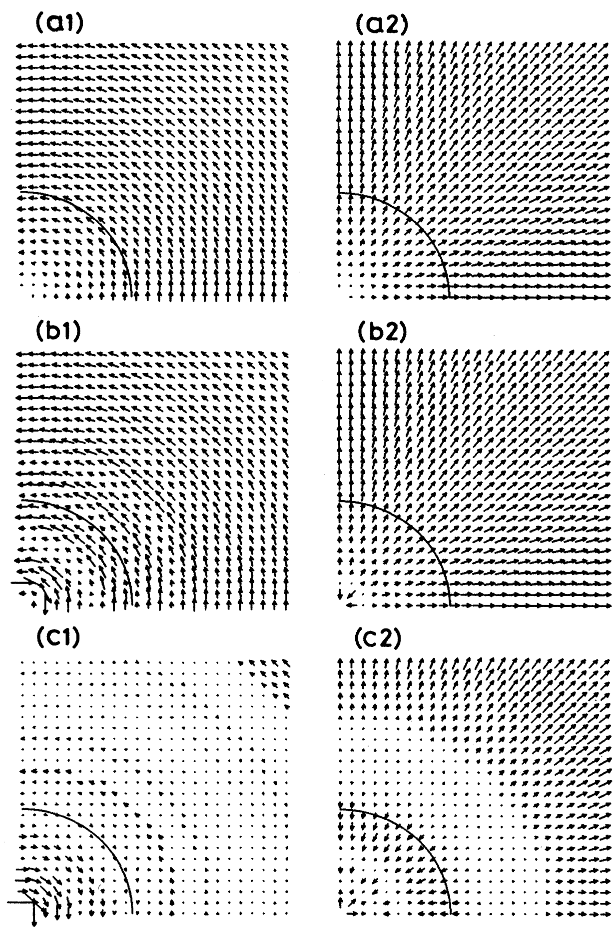

FIG. 4. Time evolution of color fields for $A=1.5$, $\kappa=1.0$, and $N=64$. (a1) and (a2) represent the configurations of the Yang-Mills field $|\mathbf{A}|=[1-G(\xi,\tau)]/\xi$ and the Higgs field $|v^{-1}\boldsymbol{\phi}|=H(\xi,\tau)/\xi$ for the static solution, respectively. Snapshots of the Yang-Mills field and the Higgs field are (b1) and (b2) for the regular stage at $\tau=120$, and (c1) and (c2) for the chaotic stage at $\tau=11\,392$, respectively. The quarter cycle stands for the boundary of the monopole core at $\xi=1$.

V. DISCUSSION AND SUMMARY

We have studied in this paper the dynamical properties of the SU(2) YMH system in the case that the field configuration depends on both space and time. From the results on the induction phenomena and the maximal Lyapunov exponents, we have found that the order-to-chaos transition occurs in the phase space near the 't Hooft–Polyakov monopole solution. Namely, this system becomes a nonintegrable one with the properties characterized by the K system at large perturbations ($A > A_c$) while it is close to a near-integrable one described by the KAM theory [11] at small perturbations ($A < A_c$). The appearance of the ordered phase is attributed to the Higgs field although our present analyses are not enough to clarify the dependence of A_c on the coupling κ. It is worth while noting that the order-to-chaos transition observed here is similar to the one found in the YMH classical mechanics [16] and the massive gauge theory with the Chern-Simons topological term in the limit of spatially homogeneous fields [17]. The nonintegrability of this system has also been shown by means of mathematical method such as the Painlevé analysis [2]. Our numerical analyses, however, clarify the dynamical structure of stochastic behavior of the SU(2) YMH system which is hard to study by such analytic methods.

It is of interest to consider the field configurations in the real time evolution under the existence of the two phases. From the asymptotic condition that $H \sim \xi$ and $G \sim 0$ as $\xi \to \infty$, Eqs. (6) and (7) dropping the time-derivative parts reduce to $G''=G$ and $h''=2\kappa h$, where $h=\xi-H$. For large ξ we have $G \sim \exp(-\xi)$ and $H \sim \xi - \exp(-\sqrt{2\kappa}\xi)$. Thus we could expect that there are different behavior between the inside ($\xi < 1$) and the outside ($\xi > 1$) of the monopole core defined by the penetration length $\xi_{\rm MC} \equiv M_A r = 1$. Figure 4 shows the time development of the YM field $|\mathbf{A}| = (1-G)/\xi$ and the Higgs field $|v^{-1}\phi| = H/\xi$ for the amplitude $A=1.5$ and the coupling constant $\kappa=1.0$. In a regular stage of Figs. 4(b1) and 4(b2), we notice sizable disturbance of fields inside the core. This comes from the coupling between the mode 32 and its adjacent modes, 31 and 33. On the other hand, after entering into a chaotic stage of Figs. 4(c1) and 4(c2), the configurations of the fields exhibit randomness in a whole region due to the excitation of all modes.

Finally, we mention that the appearance of the regular phase is also supported by the result of the analysis of the linear stability that the curvature $\delta^2 E$ derived from Eq. (8) for the small perturbations δG and δH has positive eigenvalues irrespective of the value of κ for almost all modes j. The present system is spatially inhomogeneous because of the presence of a monopole in contrast with the homogeneous system which has been used for the study of the spatiotemporal chaos. Thus it may serve for an interesting model of the Hamiltonian system [18] in the nonlinear physics.

ACKNOWLEDGMENTS

We would like to thank M. Nambu, H. Honjo, T. Hada, M. Nakayama, and S. Kawabe for many helpful discussions. One of us (T.K.) also wants to thank S. Nishiyama for encouragement and N. Saito, H. Fujisaka, H. Okamoto, and H. Mori for valuable discussions and financial support by the Saneyoshi Foundation.

[1] A. Actor, Rev. Mod. Phys. **51**, 461 (1979); S. G. Matinyan, G. K. Savvidy, and N. G. Ter-Arutunyan-Savvidy, Zh. Eksp. Teor. Fiz. **80**, 830 (1981) [Sov. Phys. JETP **53**, 421 (1981)]; B. V. Chirikov and D. L. Shepelyanskii, Pis'ma Zh. Eksp. Teor. Fiz. **34**, 1717 (1981) [JETP Lett. **34**, 163 (1981)]; W.-H. Steeb, J. A. Louw, P. G. L. Leach, and F. M. Mahomed, Phys. Rev. A **33**, 2131 (1986); T. Furusawa, Nucl. Phys. **B290**, 469 (1987); J-P. Antoine, D. Lambert, and J-A. Sepulchre, Class. Quantum Grav. **6**, 295 (1989).

[2] M. P. Joy and M. Sabir, J. Phys. A **22**, 5153 (1989).

[3] S. G. Matinyan, E. B. Prokhorenko, and G. K. Savvidy, Pis'ma Zh. Eksp. Teor. Fiz. **44**, 109 (1986) [JETP Lett. **44**, 138 (1986)]; Nucl. Phys. **B298**, 414 (1988).

[4] T. Kawabe and S. Ohta, Phys. Rev. D **41**, 1983 (1990).

[5] T. T. Wu and C. N. Yang, in *Properties of Matter Under Unusual Conditions,* edited by H. Mark and S. Fernbach (Wiley-Interscience, New York, 1969), p. 349.

[6] G. K. Savvidy, Phys. Lett. **130B**, 303 (1983).

[7] G. K. Savvidy, Phys. Lett. **71B**, 133 (1977); N. K. Nielsen and P. Olesen, Nucl. Phys. **B160**, 380 (1979); H. B. Nielsen, in *Particle Physics,* edited by I. Andrić, I. Dadić, and N. Zovko (North-Holland, Amsterdam, 1980), p. 67; P. Olesen, Nucl. Phys. **B200**, 381 (1982).

[8] G. 't Hooft, Nucl. Phys. **B79**, 276 (1974); A. M. Polyakov, Pis'ma Zh. Eksp. Teor. Fiz. **20**, 430 (1974) [JETP Lett. **20**, 194 (1974)]; P. Goddard and D. I. Olive, Rep. Prog. Phys. **41**, 1357 (1978).

[9] E. Fermi, J. R. Pasta, and S. M. Ulam, Los Alamos Science Laboratory Technical Report No. LA-1940, 1955 (unpublished).

[10] H. Hirooka and N. Saito, J. Phys. Soc. Jpn. **26**, 624 (1969); N. Ooyama, H. Hirooka, and N. Saito, *ibid.* **27**, 815 (1969).

[11] See, e.g., A. J. Lichtenberg and M. A. Lieberman, *Regular and Stochastic Motion* (Springer, Berlin, 1983).

[12] W. Mecklenburg and D. P. O'Brien, Phys. Rev. D **18**, 1327 (1978).

[13] M. Pettini and M. Landolfi, Phys. Rev. A **41**, 768 (1990).

[14] The accuracy of the eighth-order Runge-Kutta method, $\Delta\varepsilon$, is locally about $(\Delta t)^8 \sim 10^{-12}$ over a single time step. Thus we can expect naively $\Delta\varepsilon \le 10^6(\Delta t)^8 \sim 10^{-6}$ over 10^6 iterations. A rather large value of the relative error, 10^{-3}, seems to come from the numerical integration used for calculating the energy of Eq. (8).

[15] B. Julia and A. Zee, Phys. Rev. D **11**, 2227 (1975); M. K. Prasad and C. M. Sommerfield, Phys. Rev. Lett. **35**, 760 (1975); E. B. Bogomol'nyi and M. S. Marinov, Yad. Fiz. **23**, 676 (1976) [Sov. J. Nucl. Phys. **23**, 355 (1976)]. The monopole mass can be obtained by $M = 4\pi v f(\kappa)/e$, where f is the value of the integral in Eq. (8) and a slowly increasing function of κ. We obtained $f \simeq 1.00$, 1.20, 1.40, and 1.53 for $\kappa = 0.0$, 1.0, 10.0, and 50.0, respectively.

[16] S. G. Matinyan, G. K. Savvidy, and N. G. Ter-

Arutunyan-Savvidy, Pis'ma Zh. Eksp. Teor. Fiz. **34**, 613 (1981) [JETP Lett. **34**, 590 (1981)]; B. V. Chirikov and D. L. Shepelyanskii, Yad. Fiz. **36**, 1563 (1982) [Sov. J. Nucl. Phys. **36**, 908 (1982)]; G. K. Savvidy, Nucl. Phys. **B246**, 302 (1984).

[17] A. Giansanti and P. D. Simic, Phys. Rev. D **38**, 1352 (1988).

[18] See, for an example of classical chaos in a Hamiltonian system, T. Kawabe and S. Ohta, Phys. Rev. A **41**, 720 (1990).